ELSEVIER

Journal of Nuclear Materials 266–269 (1999) 495–500

journal of nuclear materials

Modeling of the dynamic ergodic divertor of TEXTOR-94

K.H. Finken [a,*], Th. Eich [a], S.S. Abdullaev [a], A. Kaleck [a], G. Mank [a], D. Reiser [a], A. Runov [b], M. Tokar [a]

[a] *Institut für Plasmaphysik, Forschungszentrum Jülich GmbH, EURATOM Association, Trilateral Euregio Cluster, D-52425 Jülich, Germany*

[b] *Institut für Laser-und Plasmaphysik, Heinrich Heine Universität, Universitätsstr. 1 D-40225 Düsseldorf, Germany*

Abstract

A Dynamic Ergodic Divertor (DED) is under construction for TEXTOR-94. The ergodization will be achieved by a set of 16 in-vessel perturbation – plus two compensation – coils located at the high field side of TEXTOR-94. The coils follow helically the resonant magnetic field lines for one toroidal turn and are individually fed outside the vessel allowing a large flexibility for possible connections. The DED-system will operate at dc or several fixed frequencies up to 10 kHz. Different and adapted modeling efforts have been undertaken both for the ergodic area and the laminar zone. The basic techniques for the ergodic zone are field line mapping and field line tracing; the analysis provides the magnetic field structure in form of Poincaré plots and the transport coefficients for the magnetic field lines. For the laminar zone a modeling is used which takes into account the typical aspects of the scrape-off layer physics. A low frequency operation of the DED will distribute the heat flux over the relatively large area of the divertor target plate. The calculations show that the high frequency operation should impose a torque on the plasma edge which is of similar size as the one imposed by tangential NBI.

Keywords: TEXTOR; Ergodic divertor; Helical divertor; Edge modeling

1. Introduction

A Dynamic Ergodic Divertor (DED) [1] is under construction for TEXTOR-94. The main reason for developing the DED is a spreading of the convective heat flux to a large plasma facing surface. The imposed magnetic field structure should (1) prevent the divertor target plate of a future reactor from overheating and excessive erosion (2) provide sufficient particle – in particular helium ash – removal (3) shield impurities – released from the walls – from penetrating into the core plasma and (4) impose a differential torque at the plasma edge which may result in improved confinement properties and delay of disruptions.

The ergodization of magnetic field lines [2–8] is created by electrical currents in perturbation coils with Fourier components resonant to magnetic surfaces inside the plasma. At sufficiently low perturbation currents, magnetic islands are generated centered at the resonant surfaces. If the perturbation current level is increased, the island chains located at different radial positions overlap. From this condition on the field lines are no longer restricted to a magnetic surface but 'diffuse' over the whole ergodic zone: A magnetic field line passing through any pre-selected starting point comes infinitely close to any target point inside the ergodic zone. This mathematical property means 'ergodization'. Since each magnetic field line connects any point inside the ergodic sea, an enhancement of the plasma transport is a characteristic feature there. Quantitative measures of the degree of ergodization are the Chirikov parameter (ratio of neighboring island widths to their distance) and related to this the field line diffusion coefficient.

Of special interest for the plasma–wall interaction are the 'open' ergodic structures. Open in this sense means that the ergodic magnetic field structure intersects the plasma boundary (divertor target plate). This 'openness' introduces a new feature, the so-called 'laminar' zone;

* Corresponding author. Tel.: +49-2461 61 5646; fax: +49-2461 61 5452; e-mail: k.h.finken@fz-juelich.de.

0022-3115/99/$ – see front matter
PII: S0022-3115(98)00541-8

the laminar zone is constituted by field lines intersecting the target plate. It will be shown below that for the TEXTOR case a large fraction of field lines intersects twice the target plate after one poloidal turn; depending on the selected condition for the ergodization, the fraction of field lines coming from the ergodic sea may be small or comparable to those with short connection length. The near field of the perturbation coils imposes a very well-ordered strike zone structure of the TEXTOR DED, helically aligned with the DED-coils. According to our modeling results the main plasma–wall interaction will take place at these divertor strike zones.

An open static ergodic divertor will therefore always face an intense localized plasma–wall interaction, similar to that of a poloidal divertor. To avoid an excessive local heating, the DED perturbation field can rotate. In this way, inhomogeneities in heat deposition are smeared out over the divertor target plate, i.e. over an area of several square meters. For smearing out the heat, a rather low rotation frequency (e.g. 50 Hz) of the perturbation field is sufficient.

The DED coils and power supplies also allow an operation in the frequency band between 1 and 10 kHz; the propagation speed of the corresponding wave pattern ranges from 240 to 7200 m/s, depending on the frequency and the coil interconnections. If – due to the rotations – the electromagnetic perturbation field exerts enough torque to the boundary plasma, it is expected that the plasma can be compressed into the pump limiter scoop (enhanced pumping) and that a velocity pattern with high shear is established at the plasma edge; these sheared patterns are often attributed a stabilizing effect. Up to now, only very few ac-ergodization systems have been described in the literature [9].

After a short description of the setup, we will first discuss the structure of the ergodic layer including the operational space. Then we will introduce a model of the laminar zone; this model is strongly oriented at conventional scrape-off layer models. Finally, we discuss the radial decay of the fast rotating field analyzing the angular momentum transferred from the wave to the plasma.

2. The DED – arrangement

The coil arrangement of the proposed DED [1] is shown in Fig. 1. It consists of a quadruple set of four helical conductors, installed on the inboard side of the TEXTOR vessel and aligned parallel to the magnetic field lines (for $\beta_{\mathrm{pol}} = 1$) at the nearby $q = 3$ surface plus two compensation coils. Taking into account the available space, the technical constraints (such as current density, skin effect, heat capacity, cooling aspects, etc.) and the physics requirements, an $m = 12$, $n = 4$ perturbation field structure has been selected. This can be achieved by using coils which cover about 30% of the inboard vessel surface on the high field side and which will be energized by a 4-phase current (up to 15 kA) at selected frequencies (dc, 50 Hz, 1 kHz and a band of 1–10 kHz). The coils can be connected in several ways and the amplitudes of the nine power supplies can be adjusted individually allowing a range of different mode structures such as the $m = 6$, $n = 2$ and $m = 3$, $n = 1$ modes. To enhance even the level of ergodization, a mode mixing at arbitrary ratios is foreseen.

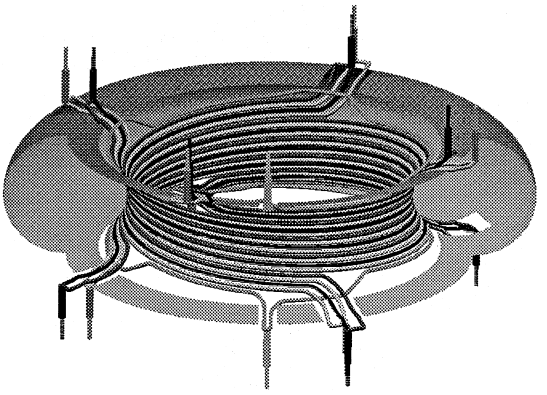

Fig. 1. Schematic sketch of the coil arrangement of the DED.

3. The ergodic layer

Field line tracing and field line mapping are basic techniques for investigating the ergodic structure. These techniques provide a picture of the areas with intact magnetic surfaces, of island structures and of ergodized regions. Beyond this, the radial displacement of the field lines has been evaluated in a statistical sense and the field line diffusion coefficient as a function of the radius has been derived.

It is found that the ergodization is not restricted to a regime close to the design point in the operational space [$\beta_{\mathrm{pol}} = 1$, $r(q_{\mathrm{res}} = 3) = 0.42$ m]; indeed, the ergodization grows even when lowering β_{pol} while keeping the resonant radius constant. The resonant radius can be adjusted at a given β_{pol} by the plasma current; in this way the ergodic zone can be shifted either more towards the plasma edge or more inwards in the range $0.9 \leqslant r/a \leqslant 1$ keeping a sufficient degree of ergodization.

The perturbation field amplitude decays proportionally to $(r/r_{\mathrm{coil}})^{m_{\mathrm{eff}}}$ (due to the shallower magnetic field line pitch at the HFS, m_{eff} is larger than the poloidal mode number if the coils are located at the HFS; for the $m/n = 12/4$ mode it amounts to about $m_{\mathrm{eff}} \approx 20$); therefore the ergodization strength decays strongly when the resonance zone is shifted deeper into the plasma.

The above mentioned individual adjustment of the nine power supplies allows the superposition of different external base modes. To minimize the interaction with the core plasma, high m/n (e.g. $m/n = 12/4$) are preferred; for the given coil arrangement, mode numbers $m \leqslant 8$ can be neglected. This choice creates in a favorable way many small islands instead of a few islands with large poloidal extent. A problem, however, is the rapid decay of the perturbation amplitude with the distance from the coils. This rapid decay can be compensated by an admixture of the $m/n = 6/2$ mode to the base 12/4 mode. By such a mixing, the perturbation field amplitude and its penetration depth into the plasma become partially decoupled. This mode mixing will provide the highest ergodization levels in TEXTOR-94 with a Chirikov parameter above four at the plasma edge and above one for over 6 cm. To our judgment, the maximum tolerable admixture of the 6/2 mode will amount to about 30% because from this value on the $q = 2$ surface will merge into the ergodic sea. Fig. 2 shows a Poincaré plot for this 15% admixture of the 6/2 mode and Fig. 3 gives the radial dependence of the Chirikov parameter for two different mixing ratios. The analysis was performed both by field line tracing and by mapping; both methods agree excellently.

In the ergodic layer, the Chirikov parameter and the field line diffusion coefficient (D_{FL}; dimension: m^2/m; relation to normal diffusion coefficient: $D = D_{\mathrm{FL}} \times v_{\mathrm{th}}$) are related in a monotonous way. On the other hand, the diffusion coefficient can be studied by computing the

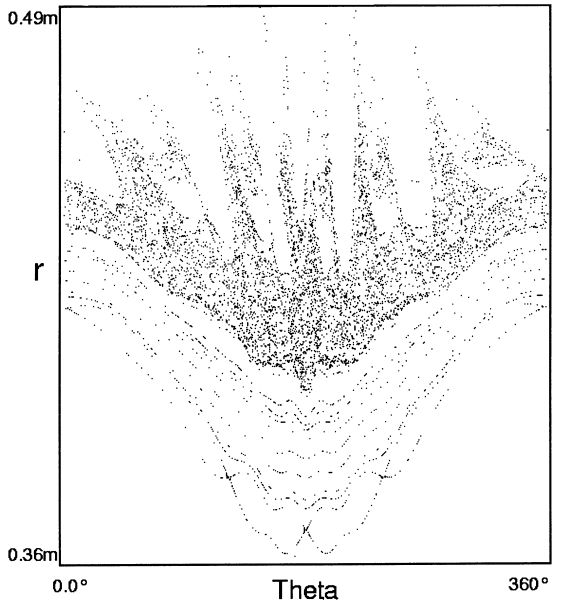

Fig. 2. Poincaré plot of an admixture of 15% of the $n = 6/2$ mode to the base 12/4 mode. The resonant radius is located at $r_{\mathrm{res}} = 46$ cm and the perturbation coil current $I_{\mathrm{pert}} = 15$ kA.

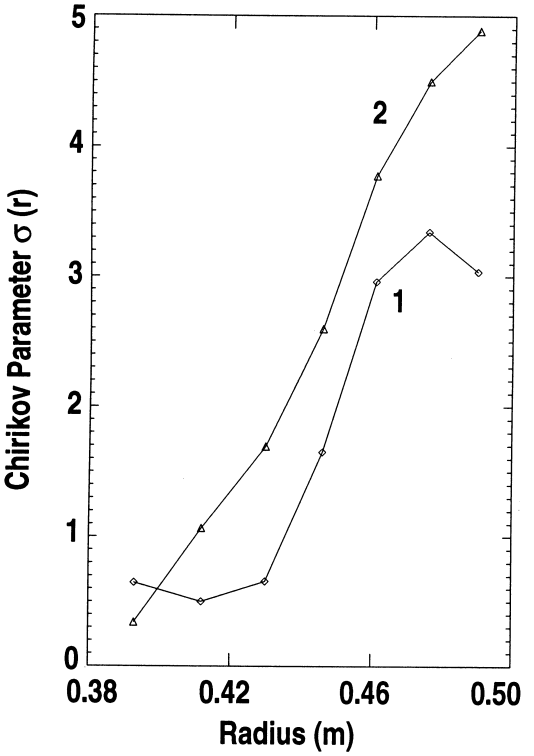

Fig. 3. Chirikov parameter for mixing ratios of 0% (1) and 15% (2). The parameters are the same as in Fig. 2.

mean radial displacement $\sigma_{ro}(k) = \langle (r_k - r_o)^2 \rangle$ for k mapping steps. This quantity is growing at the interval $k \leqslant k_c$ and rapidly decaying for $k \gg k_c$ because the field lines leave the ergodic zone [10]. The local field line diffusion coefficient was deduced by calculating $\sigma_r(k)$ in the initial linear regime and relating D_{FL} by $D_{\mathrm{FL}} = \sigma_r(k)/2L$ where L is the length of the field lines $L = \pi R_o k/2$. This definition of D_{FL} can be used both in the ergodic layer and in the laminar zone. Fig. 4 shows the field line diffusion coefficient for the same conditions as Fig. 3. Although in Fig. 3 the Chirikov parameter grows towards the plasma edge, the field line diffusion coefficient shows distinct maxima: Coming from the plasma interior, D_{FL} grows with the increasing Chirikov parameter as expected. The decrease beyond the maximum (i.e. more at the outside) is explained by a change of the character of the transport: the transport changes from a diffusion dominated process to a convection dominated process and this zone will be dominating in the laminar zone of the TEXTOR-DED.

4. The laminar zone

Topological investigations of the connection lengths of the magnetic field lines in the plasma edge have elu-

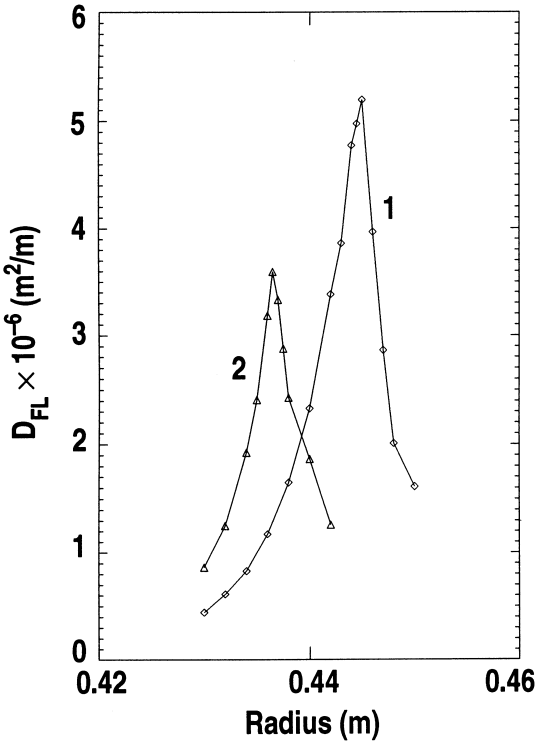

Fig. 4. Field diffusion coefficient for the same conditions as in Fig. 3. The laminar zone is the area right of the maximum of the curves.

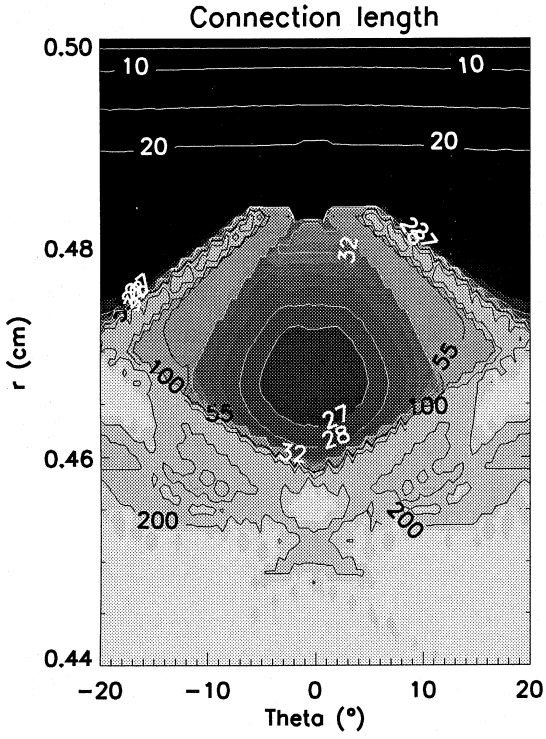

Fig. 5. Topology of the field line connection length of the laminar zone plotted near the outer equatorial midplane. The different connection lengths are marked by iso-contour-lines.

cidated the structure of the laminar zone. It has been shown [11] that – despite of the strong ergodization – rather large continuous areas exist where the connection length of the field lines has similar properties: We find 4×1 continuous areas (4 times because of the four fold toroidal symmetry) where field lines intersect the walls twice after one poloidal turn; we find 4×2 continuous areas with a connection length of two turns. The area of even longer connection lengths is strongly decreasing. Already the third order area is so small that the Larmor orbits of the ions mix these areas with the other higher order areas and with the ergodic sea. Fig. 5 shows an example of these topological structures. For easiest representation we have chosen a 2-D cut near the outer equatorial midplane (coordinates: radius and poloidal angle) and we have marked the characteristic areas in different gray shades. The characteristic length of a poloidal turn is about 30 m. It is interesting to note the small band between the single and double turn connection area which contains field lines of different lengths closely mixed; this band connects the ergodic sea (plotted dotted white) with the walls.

Despite the strong ergodization, the large continuous structures of single and double poloidal connection lengths suggest to treat the plasma edge in a similar way as the SOL of a poloidal divertor. The two areas have a relatively simple boundary with respect to the ergodic zone and the small scale zones of finite but relatively long connection lengths. For our modeling, this boundary is treated in the same way as the separatrix of a poloidal limiter: In a first approximation it is assumed that the particles and the power (minus the radiative fraction) brought into the plasma cross the boundary and diffuse across the magnetic field into the laminar zone. Just as in the SOL, the transport along the field lines is treated convectively and perpendicular to the field lines diffusely. The electron heat conductivity is assumed to be infinitely high leading to a constant T_e along the field lines; the temperature drop only occurs in the Langmuir sheath in front of the divertor target plates. The density, the ion temperature and the velocity along the magnetic field is calculated from the continuity equation, momentum equation and the ion heat conduction equations. The perpendicular transport is treated by a finite element solver (PDE2D). The parallel and perpendicular transports are calculated iteratively (operator splitting) until convergence.

The main difference to the conventional solutions arises in the area of double poloidal connection length. Here it has to be analyzed how the different points in

Fig. 5 are interconnected. The interconnection leads to an exchange of fluxes along the field lines. Since predominantly field lines from smaller radii are connected to those laying more outwards, particles and energy are transported more effectively by convection than would occur by diffusion alone. Therefore the wedge shaped area of double connection length contributes in an enhanced way to the transport. A result of the temperature modeling is shown in Fig. 6.

5. Dynamic aspects

High frequency aspects of the DED-field have been analyzed in cylindrical approximation. The only relevant component of the vector potential of the perturbation field is the one in axial direction [12]. It has been shown [13] that in a good approximation the 'low frequency' electromagnetic wave of the DED propagates as a vacuum field in the area between coils and resonance layer. In the tearing mode theory [14], the phase velocity in this outer layer is the Alfvén velocity times the sine of the angle between the local magnetic field and the magnetic field at the resonance layer.

At the resonance layer we describe the plasma by an annulus of finite resistivity which is given by the local electron temperature (skin effect) [15]. An uncertainty is the question: which radial width of the segment (2ε) is the relevant one? One reasonable choice is the island width derived from the Poincaré plots which gives typically a value of $2\varepsilon = 2.5$ cm. An example of the radial dependence of the vector potential $a_z(r)$ is shown in Fig. 7 for $m_{\text{eff}} = 20$ (12/4 mode; diamonds) and 5 (3/1 mode; line) at a frequency of 10 kHz. The resistive layer is located in between $r = 0.42$ m and $r = 0.445$ m. Between the coils and resonant plasma zone, the B_φ-component (i.e. $\mathrm{d}a_z/\mathrm{d}r$) drops by a factor of 20 for an effective azimuthal mode number of $m_{\text{eff}} = 20$ while the drop of the $m_{\text{eff}} = 5$ mode can be neglected. Inside the resistive layer, the field component drops by more than 2 orders of magnitude. Therefore, if the assumption about the current carrying channel is correct it can be expected that the 10 kHz modes are well shielded in the resonant layer and do not create detrimental islands deep inside the plasma.

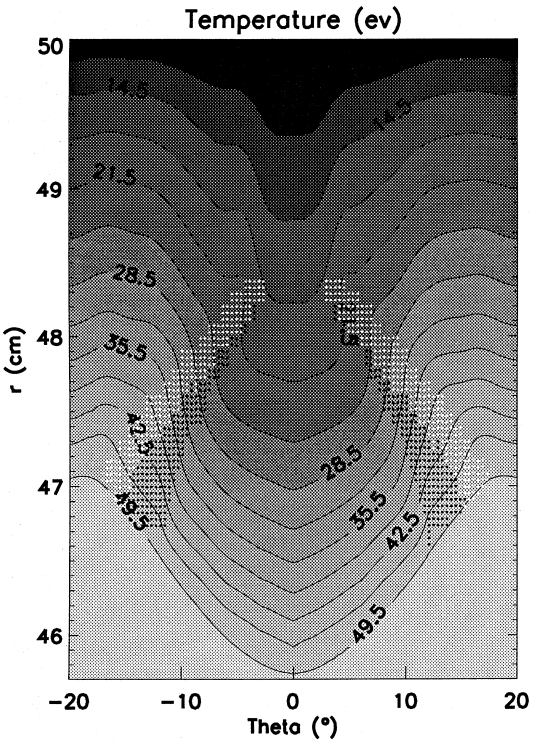

Fig. 6. Calculated temperature distribution in the plane of Fig. 5. The field lines in the black dotted and white dotted areas intersect the divertor target plate after two toroidal turns. From the black dotted area, heat and particles are transported convectively to the white dotted area.

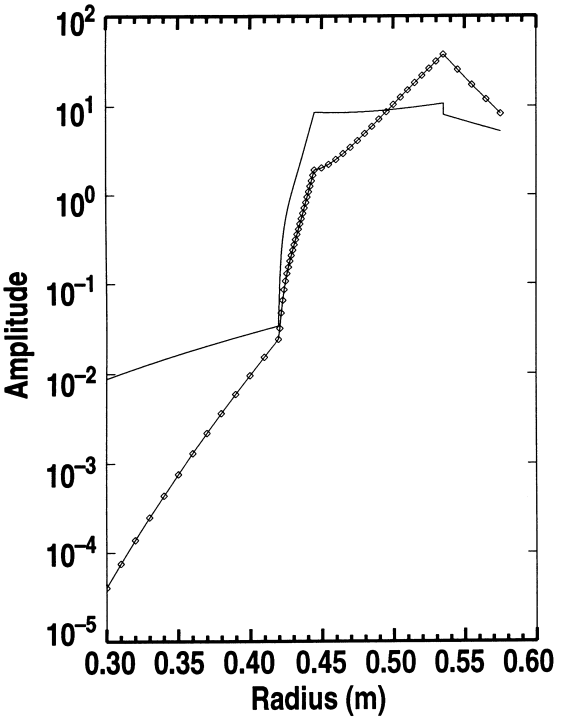

Fig. 7. Perturbation field amplitudes are shown as a function of the radius at $f = 10$ kHz and for an electron temperature of 50 eV. The diamonds represent the $m_{\text{eff}} = 20$ mode and the line the $m_{\text{eff}} = 5$ mode. The perturbation field propagates as in vacuum with the exception of a 'resonance' ring between $0.42\ \text{m} < r < 0.445\ \dagger\ \text{m}$; there skin-type penetration is assumed.

A second reasonable assumption about the width of the shielding current channel is the width of tearing modes. This is given by equating the skin depth ($\delta^2 = 1/\sigma\omega\mu_o$) with the characteristic length of the poloidal Alfvén wave $v_{A\text{-pol}}/\omega$ ($v_{A\text{-pol}}$ is zero at the resonance layer and grows nearly linearly with the distance) and yields a value of about $2\varepsilon = 1$ mm. Although the decay of the field amplitude within this narrow layer is small, the phase difference between the inner and outer solution reaches values of about 60° (for $T_e = 50$ eV).

The analytical model allows the evaluation of the power (Poynting vector $\langle S_r \rangle$) and angular momentum ($\langle T_z \rangle / \langle S_r \rangle = m_{eff}/\omega$) transfer to the plasma. Taking into account the fractional coverage of the coil system with respect to the plasma surface, the following values are obtained for $\langle T_z \rangle$ at full coil current and for a current layer of 2.5 cm width: $\langle T_z \rangle = 2$ Nm ($m_{eff} = 20$), 12 Nm ($m_{eff} = 10$) and 11 Nm ($m_{eff} = 5$). The thinner layer resulting from the tearing mode approximation gives torques which are even a factor of 3 higher and is consistent with an ac-motor model [16]. Even if a poloidal rotation of the plasma is forbidden by neoclassical arguments, the toroidal projection is about as large as the torque imposed by the neutral beams. A combined operation of the high frequency DED with NBI will allow one to impose interesting differential rotations between the plasma edge (action of the DED) and the core (by NBI).

6. Conclusions

The modeling of the DED has shown its extremely interesting features. The ergodization layer can be varied in radial location, in width, and in strength of ergodization. The Chirikov parameter reaches values of >4 and provides sufficiently strong ergodization. The field line diffusion coefficient is derived from the statistical properties of the field line displacement. Different from the conventional quasi-linear theory, the diffusion coefficient can have a local maximum which separates the diffusion dominated part from the convection dominated laminar zone.

The description of the laminar zone has been refined by a model which is related to the conventional SOL divertor-models. Similar to the SOL of a divertor, the laminar zone contains large areas with the property that all field lines connect the divertor target plate after one poloidal turn. In addition to this, there also exist areas with multiples of this connection length. Progress of the modeling has been made by taking into account the exchange fluxes in these layers which, on the average, lead to an enhanced outward transport.

The effect of the rotating field of the dynamic ergodic divertor is described by a resistive shell model. The shell is located around the resonance layer. The radial width of the shell may be discussed. If one assumes that its width is given by the island width of the Poincaré plots, one can derive that at 10 kHz the resonance layer shields well the interior from the perturbation field. If resistive tearing modes determine the current layer width, then the interior is not effectively shielded; however, the rotating DED field transfers a torque to the plasma which is of the same order as the one by NBI. Therefore interesting differential rotations may be applied by the combination of the DED and NBI.

References

[1] Dynamic Ergodic Divertor (special issue), Fusion Eng. Des. 37 (1997) 335–448 (15 contributions).
[2] A.J. Lichtenberg, M.A. Liebermann, Regular and Stochastic Motion, Springer, New York, 1983.
[3] A.B. Rechester, M.N. Rosenbluth, Phys. Rev. Lett. 40 (1978) 38.
[4] A. Grosman, T.E. Evans, Ph. Ghendrih et al., Plasma Phys. Control. Fusion 32 (1990) 1011.
[5] Ph. Ghendrih, A. Grosman, H. Capes, Plasma Phys. Control. Fusion 38 (1996) 1653.
[6] T.E. Evans, S.J. deGrassie, G.L. Jackson et al., J. Nucl. Mater. 145&146 (1986) 812.
[7] S.C. McCool, A.J. Wooton, A.J. Ademir et al., Nucl. Fusion 29 (1989) 547.
[8] T. Shoji, H. Tamai, Y. Miura et al., J. Nucl. Mater. 196–198 (1992) 296.
[9] S. Takamura, Y. Shen, H. Yamada et al., J. Nucl. Mater. 162–164 (1989) 643.
[10] S.S. Abdullaev, K.H. Finken, A. Kaleck, K.H. Spatschek, Phys. Plasmas 5 (1998) 196.
[11] K.H. Finken, T. Eich, A. Kaleck, Nucl. Fusion 38 (1998) 515.
[12] K.H. Finken, Nucl. Fusion 37 (1997) 583.
[13] D.W. Faulconer, R. Koch, Fusion Eng. Des. 37 (1997) 399.
[14] J. Rem, T.J. Schep, Plasma Phys. Control. Fusion 40 (1998) 139.
[15] R. Fitzpatrick, Nucl. Fusion 33 (1993) 1049.
[16] T.H. Jensen, A.W. Leonard, A.W. Hyatt, Phys. Fluids B5 (1993) 1239.